Journal of Organometallic Chemistry, 438 (1992) 183–194
Elsevier Sequoia S.A., Lausanne
JOM 22763

The reaction between ferrocenyllithium and trimethylacetylchloride to form either trimethylacetylferrocene or 1,1′-bis(ferrocenyl)-2,2′-dimethylpropan-1-ol, an unusual hydrogen bonded dimer

Hemant K. Sharma, Francisco Cervantes-Lee and Keith H. Pannell
Department of Chemistry, The University of Texas at El Paso, El Paso, Texas 79968-0513 (USA)
(Received December 17, 1991)

Abstract

The addition of ferrocenyllithium, FcLi, to trimethylacetylchloride, Me_3CCOCl, yields trimethylacetylferrocene, $FcCOCMe_3$, (I), in 77% yield, whereas the reverse addition results in the isolation of 1,1′-bis(ferrocenyl)-2,-2′-dimethylpropan-1-ol, $Fc_2C(CMe_3)OH$, (II), a very sterically hindered alcohol, in 62% yield. The conversion of I to II via treatment with FcLi is a facile process occurring in 83% yield. The spectroscopic and structural data on I show it to be less basic than its Si and Ge analogs, but structurally almost identical in terms of C=O bond length *etc*. The single crystal structural analysis of the α-ferrocenylcarbinol (II) shows that it forms discrete cyclic dimers, with the component molecules held together by two symmetrical non-linear hydrogen bonds, a relatively rare type of intermolecular H-bonding.

Introduction

Recently, we reported some chemical and structural aspects of (ferrocenylacyl)-silanes and -germanes [1,2]. In order to compare the spectral and structural features of these acyl Si and Ge compounds with their C analog we have attempted to synthesize $FcCOCMe_3$ (I) *via* the reaction of ferrocenyllithium and Me_3CCOCl. We wish to report the results of such a study involving the formation of the desired product, as well as a further reaction product from addition of FcLi to the new acylferrocene, *i.e.* $Fc_2C(CMe_3)OH$ (II), together with single crystal structural studies of both I and II. Subsequent to the completion of this study, complex I was reported by Bell and Glidewell from the Friedel–Crafts reaction of ferrocene with trimethylacetylchloride [3].

Correspondence to: Dr. K.H. Pannell.

Results and discussion

Trimethylacetylferrocene was obtained by the slow addition of monolithioferrocene to a THF solution of trimethylacetyl chloride at low temperature (eq. 1):

$$Fc^{-}Li^{+} + Cl{-}\overset{\overset{O}{\|}}{C}{-}CMe_3 \xrightarrow[THF]{-25^{\circ}C} Fc(CO)C(CH_3)_3 \quad (1)$$

(I)

Reverse addition, *i.e.* addition of the trimethylacetyl chloride to ferrocenyllithium, leads to a different complex in good to moderate yield as the sole product, $Fc_2C(CMe_3)OH$ (eq. 2):

$$Cl{-}\overset{\overset{O}{\|}}{C}{-}CMe_3 + Fc^{-}Li^{+} \xrightarrow[THF]{-25^{\circ}C} Fc_2C(CMe_3)OH \quad (2)$$

This unexpected product is apparently formed via a rapid addition of FcLi, which is in excess, to I formed in the initial stages of the reaction to form the alkoxide ion which subsequent to aqueous work yields II, eq. 3. This scheme was proven *via* independent synthesis, eq. 4.

$$Fc^{-}Li^{+} + Cl{-}\overset{\overset{O}{\|}}{C}{-}CMe_3 \longrightarrow [Fc{-}\overset{\overset{O}{\|}}{C}{-}CMe_3] \xrightarrow{Fc^{-}Li^{+}}$$

$$Fc{-}\overset{\overset{O^{-}Li^{+}}{|}}{\underset{\underset{Fc}{|}}{C}}{-}CMe_3 \xrightarrow{H_2O} Fc{-}\overset{\overset{OH}{|}}{\underset{\underset{Fc}{|}}{C}}{-}CMe_3 \quad (3)$$

$$FcCOCMe_3 + Fc^{-}Li^{+} \xrightarrow[2.\ H_2O]{1.\ -25^{\circ}C/THF} Fc_2C(CMe_3)OH \quad (4)$$

The secondary attack of $Fc^{-}Li^{+}$ upon the carbonyl group does not occur with the corresponding Si and Ge analogs which are unreactive with respect to nucleophilic attack at the C=O group.

Spectroscopic and structural analysis of I

The infrared spectrum of I exhibits a carbonyl stretching frequency at 1651 cm^{-1} in CH_2Cl_2, 73 cm^{-1} and 57 cm^{-1} higher than the respective silicon and germanium analogs, $FcCOEMe_3$ [1,2,4]. This is consistent with the relative basicities as measured by H-bonding studies to phenol in carbon tetrachloride solution. The shifts between the νOH of H-bonded phenol and free phenol in the presence of $FcCOEMe_3$, E = C, Si and Ge presented in Table 1 show that the order of base strength is $FcCOSiMe_3 > FcCOGeMe_3 > FcCOCMe_3 \gg PhCOCMe_3$. Thus, replacement of the α-carbon by silicon or germanium increases the availability of electrons on the carbonyl oxygen and is responsible for the higher basicity of (ferrocenylacyl)silanes and -germanes. Both the ferrocenyl and silyl/germyl groups, have a basicity enhancing effect.

Table 1

K_F for phenol/acyl compound, $\Delta\nu$ for phenol ν(OH)

Compound	K_F	$\Delta\nu$ (cm^{-1})
$PhCOCMe_3$	–	162 (ref. 10)
$FcCOCMe_3$	22.5	207 (this work)
$FcCOGeMe_3$	21.6	235 (ref. 2)
$FcCOSiMe_3$	32.0	261 (ref. 1)

Trimethylacetylferrocene (I) exhibits a ^{13}C carbonyl-carbon resonance at 208 ppm which is 27–29 ppm lower than the silicon and germanium analogs indicating that Si and Ge have a strong deshielding effect on the carbonyl–carbon resonance [1,2].

The molecular structure of I is shown in Fig.1, and selected bond lengths and angles are listed in Table 2. The C=O bond length of 1.220(5) Å is comparable to that of the related silicon and germanium analogs when the experimental error is taken into account and also to the values of 1.220(3) Å reported for $FcCOCH_3$ [5], 1.221(7) Å for $(CO)_2NOCr(\eta^5\text{-}C_5H_4)CH_2(\eta^5\text{-}C_5H_4)Fe(\eta^5\text{-}C_5H_4)C(O)(\eta^5\text{-}C_5H_4)Cr(CO)_2NO$ [6], and 1.203(7) Å for $FcCOC_6H_5$ [7]. The angles at the carbonyl group (119.1°, 117.9°, 123.0°) are also comparable to those reported for the related acylsilane and -germane. Of these three angles, C(1)–C(11)–C(12) is the greatest and, when coupled with the dihedral angle between the cyclopentadienyl ring plane and the C–C=O plane of 11.5°, support earlier conclusions that the steric bulk of the ferrocenyl group has a dominant effect in the ferrocenylacyl system [1,2,4].

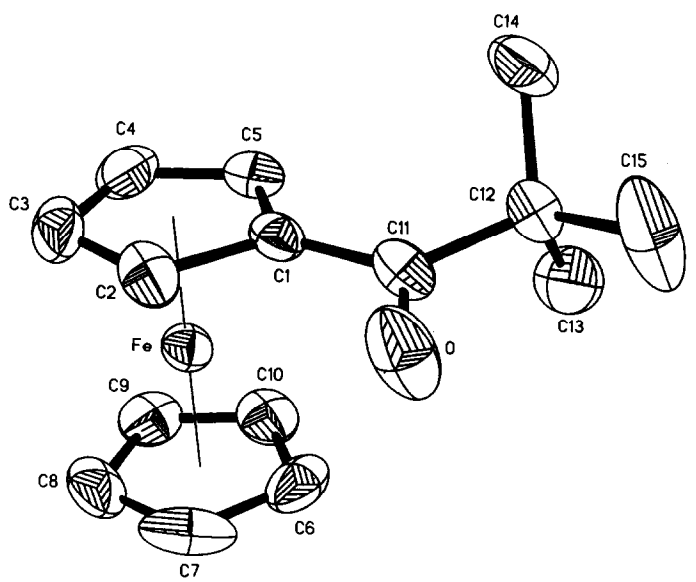

Fig. 1. Molecular structure of I.

Table 2

Comparison of bond lengths (Å) and angles (°) about the ketone group and ring stagger angles

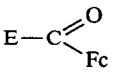

(E = C, Si, Ge)

Bond lengths/angles	$FcCOCMe_3$	$FcCOSiMe_3$	$FcCOGeMe_3$
C–O	1.220(5)	1.231(6)	1.225(9)
Fc–C(CO)	1.479(5)	1.475(7)	1.479(10)
E–C	1.528(5)	1.940(5)	1.998(7)
E–C–Fc	123.0(3)	123.6(4)	122.6(5)
E–C–O	117.9(3)	117.2(4)	117.8(5)
O–C–Fc	119.1(3)	119.2(5)	119.6(7)
ring stagger	4.8	2	4.5

Spectroscopic and structural analysis of II

The infrared spectra of II at different concentrations in CCl_4, 1×10^{-3} to 1×10^{-2} mol/l, exhibit only a single sharp band at 3559 cm^{-1} (3549 cm^{-1}, KBr) associated with the hydroxyl group. We were unable to detect any lower frequency bands. Early studies by Trifan and Backsai [8] and a subsequent series of papers by Epstein and coworkers [9] concerned the H-bonding characteristics of a number of ferrocenyl alcohols and determined that in addition to expected intermolecular H–O ··· H–O bonding, intermolecular O–H ··· π, and intramolecular O–H ··· Fe bonding were also important and indeed sometimes predominated. Based upon their analysis of O–H stretching frequencies ν (free O–H) for ferrocenylcarbinols should be about 3620 cm^{-1}, suggesting that the single band observed for II at 3559 cm^{-1} is associated with the intramolecular O–H ··· Fe type of interaction. We have attempted to disrupt this bonding by addition of pyridine with no success. Apparently, the great steric bulk at the alcohol C atom forces this unique type of H-bond to the metal center at the expense of all other types. Furthermore such bulk precludes the presence of any free OH, placing the C–O–H group into a conformation where the only location for the hydrogen atom involves the interaction with the central Fe atom. This idea was also suggested as a result of molecular mechanics calculations [9b].

In order to obtain more structural information about the hydrogen bonding, the X-ray structure was determined. The structure, Fig. 2a, contains two independent molecules in the asymmetric unit which are identical in conformation and bond lengths. This is illustrated in Fig. 2b where the two structures are superimposed. Relevant bond lengths and angles are given in Table 3. Contrary to the expectation of a O–H ··· Fe type of interaction, it is clear that the H^1 atom attached to the O(1) atom is oriented away from the iron atom Fe(2). The intramolecular Fe(2)–H^1 contact distance is 3.326 Å, and the non-bonding distance Fe(2)–O(1) is 3.646 Å and this clearly rules out the possibility of any intramolecular interaction of Fe(2) with the hydroxyl group.

Closer inspection of the structure reveals the dimeric nature of II from which it is possible to discern the nature of the H-bonding in the solid state. A stereoview of the H-bonded dimer is presented in Fig. 3. The intermolecular contact distances H1A ··· O1B and H1B ··· O1A are equivalent at 2.287 Å and O–H ··· O linkages

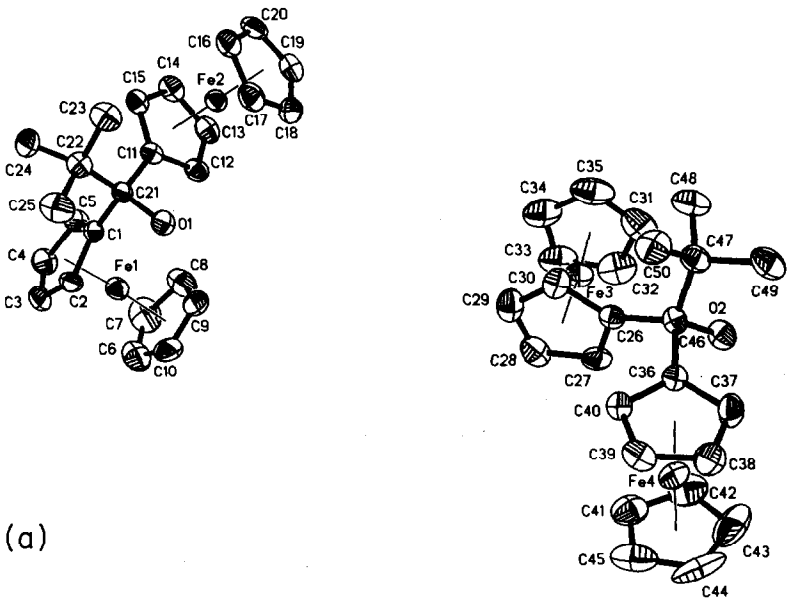

(a)

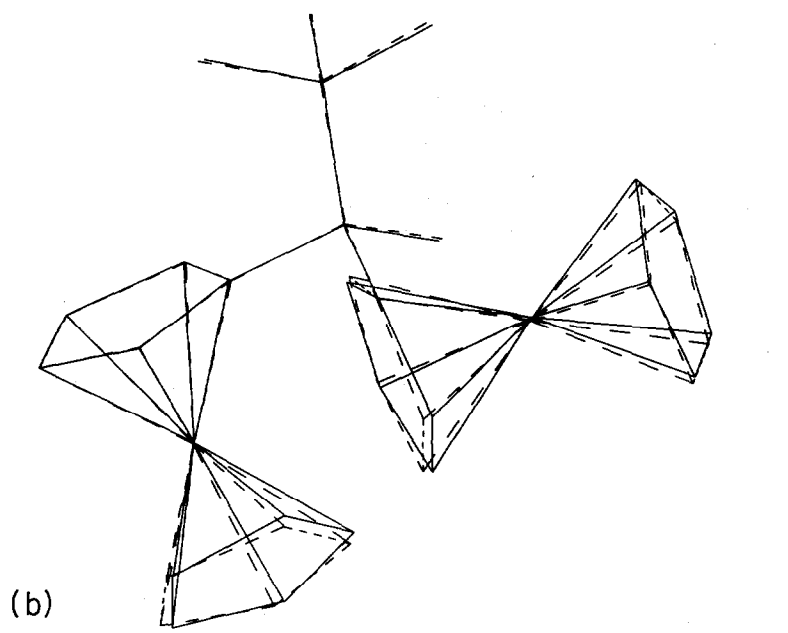

(b)

Fig. 2. (a) Asymmetric unit of II. (b) Comparison of the two molecules in the asymmetric unit of II.

are bent with an angle of 125°, while the O · · · O distance is 2.72 Å. Such values are well within the acceptable limits for intermolecular H · · · bonding, and are remarkably similar for example to those observed in 3′-amino-3′-deoxythymidine, a precursor to a non-competitive inhibitor of HIV-1 reverse transcriptase [17]. Presumably, the steric bulk of ferrocenyl and t-butyl group prevents the linear type

Table 3

Selected bond lengths (Å) and angles (°) for II

C21–O1	1.432(5)	C46–O2	1.442(4)
C21–C22	1.579(6)	C46–C47	1.584(7)
C21–C1	1.524(6)	C46–C26	1.532(6)
C21–C11	1.542(6)	C36–C36	1.520(6)
O1–C21–C11	108.6(3)	C22–C21–C1	109.5(3)
O1–C21–C1	106.2(3)	C11–C21–C1	107.2(4)
O1–C21–C22	109.8(4)		

of intermolecular hydrogen bonding O–H · · · O between the two individual molecules in the unit cell. Such carbinol dimers are reported as well as trimers and tetramers [12,14–16]. Clearly the solid state structures of alcohols may take on a variety of H-bonded oligomers reminiscent of H_2O structures. For example, Herndon and Radhakrishnan recently showed [13] that H_2O dimers can exist as linear, cyclic or bifurcated forms, and that the calculated energies of these are very similar and indeed the relative calculated stabilities vary according to the type of calculation.

Our results with II differ considerably from other α-metallocenylcarbinols studied by Epstein *et al.* in which α-ferrocenylcarbinols primarily form OH · · · π and OH · · · *M* intramolecular hydrogen bonds as observed both by infrared and single crystal structure determination [9a,e]. For example, in the case of $(\eta^5$-$C_5H_5)Fe(\eta^5$-$C_5H_4)CH(OH)(\eta^6$-$C_6H_5Co_4(CO)_9$, which exhibits intramolecular O-H · · · Fe bonding via infrared spectroscopy, the same structure is observed in the solid state; the Fe–H contact is 2.9(1) Å, Fe–O is 3.466(5) Å, and the Fe–H–O angle is 113(8)°. In the case of complex II there is a clear change from intramolecular to intermolecular H-bonding upon changing from solution to the solid state.

Experimental

All manipulations were carried out in dry, oxygen-free solvents under dinitrogen. $[(\eta^5$-$C_5H_5)Fe(\eta^5$-$C_5H_4)]^-Li^+$ was synthesized, using a literature procedure

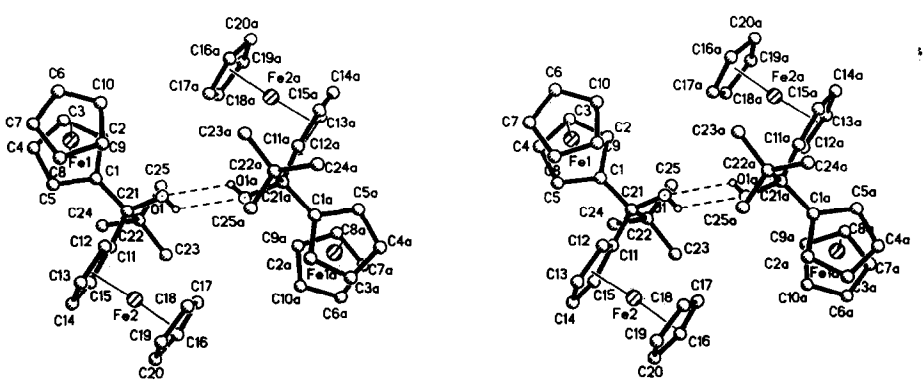

Fig. 3. Stereoview of the H-bonded dimer of II.

[10], from chloromercurioferrocene (Strem Chemicals, Newburyport, MA). Trimethylacetyl chloride was used as obtained from Aldrich Chemicals, Milwaukee, WI.

NMR spectra were recorded on a Bruker NR 200 MHz spectrometer and infrared spectra were recorded on a Perkin–Elmer 1600 FT IR spectrophotometer. Elemental analyses were performed by Galbraith Laboratories, Knoxville, TN.

Synthesis of trimethylacetylferrocene, I

Monolithioferrocene, prepared from 6.3 g (15 mmol) of chloromercurioferrocene and 31.0 mmol of 1.6 *M* n-butyllithium in 60 mL of THF, was added slowly to a 20 mL THF solution of trimethylacetyl chloride (1.9 g, 15 mmol), maintained at −25°C. The addition was conducted over a period of an hour. The mixture was stirred at low temperature for 30 minutes and was then stirred for a further 20 h at room temperature. At this time the mixture was hydrolyzed. The organic layer was extracted with 150 mL of hexane and dried over $MgSO_4$. After filtration, the hexane was evaporated on a rotary evaporator and di-n-butyl mercury was distilled on a water bath at 60–62°C/0.2 mm Hg. The dark red residue was recrystallized from hexane to yield 3.1 g, 11.5 mmol (77%) of I, m.p. 89–90°C. Anal. Found: C, 66.25; H, 6.70%. Calcd.: C, 66.66; H, 6.66. IR (cm^{-1}) CCl_4 ν(C=O) 1660.5. ^1H NMR (C_6D_6) δ (ppm) 1.23 (9H, s, $C(CH_3)_3$); 3.94 (5H, s, Fc); 4.09 (2H, t, Fc); 4.72 (2H, t, Fc). ^{13}C NMR (C_6D_6) δ(ppm) 28.26 ($C(CH_3)_3$); 44.12 ($C(CH_3)_3$); 69.96, 71.19, 71.25, 77.50 (Fc); 208.13 (C=O).

Synthesis of 1,1'-bis (ferrocenyl)-2,2'-dimethylpropan-1-ol, II

Trimethylacetyl chloride (1.81 g, 15 mmol) in 20 mL of THF was added dropwise at −25°C to 60 mL of a THF solution of monolithioferrocene prepared from 6.3 g, 15 mmol of chloromercurioferrocene and 31.0 mmol of 1.6 *M* n-butyllithium. The mixture was stirred for 30 minutes at low temperature and then allowed to warm to room temperature. After stirring for an additional 20 h, the volatile materials were removed under vacuum. The residue was extracted with 100 mL of hexane and filtered. The filtrate was poured into three times its volume of water. The organic layer was extracted twice with hexane, washed repeatedly with water, and dried over sodium sulfate. The solvent was evaporated. Vacuum sublimation of the residue at 50°C/0.2 mmHg removed di-n-butyl mercury. The residue was recrystallized twice from hexane to produce orange-red crystals of II, 2.12 g, 4.65 mmol (62%), m.p. 152–153°C. Anal. Found: C, 65.94; H, 6.22. Calcd.: C, 65.76; H, 6.14%. IR (cm^{-1}) CCl_4 ν(OH) 3559; (3549 in KBr). ^1H NMR ($CDCl_3$) δ (ppm) 1.07 (s, 9H, C–$(CH_3)_3$); 2.42 (s, 1H, –C–*OH*); 4.05–4.14, 4.23–4.24 (m, s, 18H,Cp). ^{13}C NMR ($CDCl_3$) δ (ppm) 28.0 (q, J = 46.2 Hz, $-C(CH_3)_3$); 39.5(s, $-C(CH_3)_3$); 66.5, 67.0, 68.6, 69.5, 70.3 (Cp); 98.5 (s,–*C*–OH).

Reaction of monolithioferrocene with trimethylacetylferrocene

To 3.0 g (11 mmol) of trimethylacetylferrocene (I) dissolved in 60 mL of THF maintained at −25°C was added a 40 mL THF solution of monolithioferrocene obtained from 4.68 g, 11 mmol of chloromercurioferrocene and 23 mmol of 1.6 *M* n-butyllithium. The mixture was stirred at low temperature for 1 h and then at room temperature for 20 h. At this time the mixture was hydrolyzed and the organic layer was extracted with 100 mL of hexane and dried over $MgSO_4$. After

Table 4a

Crystal data and refinement details for complex I

Empirical formula	$C_{15}H_{18}FeO$
Color; habit	Red fragment
Crystal size (mm)	$0.24 \times 0.32 \times 0.30$
Crystal system	Monoclinic
Space group	$P2_1/n$
Unit cell dimensions	$a = 6.005(3)$ Å
	$b = 15.835(7)$ Å
	$c = 13.735(5)$ Å
	$\beta = 94.02(3)°$
Volume	1302.8(10) Å^3
Z	4
Formula weight	270.1
Density (calc.)	1.377 Mg/m^3
Absorption coefficient	1.137 mm^{-1}
$F(000)$	568
Diffractometer Used	Siemens R3m/V
Radiation	Mo-K_α ($\lambda = 0.71073$ Å)
Temperature (K)	298
Monochromator	Highly oriented graphite crystal
2θ Range	3.5 to 45.0°
Scan type	ω
Scan speed	Variable; 3.00 to 20.00°/min. in ω
Scan range (ω)	1.30°
Background measurement	Stationary crystal and stationary counter at beginning and end of scan, each for 25.0% of total scan time
Standard reflections	3 measured every 100 reflections
Index ranges	$0 \leqslant h \leqslant 6$, $0 \leqslant k \leqslant 17$, $-14 \leqslant l \leqslant 14$
Reflections collected	2002
Independent reflections	1724 ($R_{int} = 1.40\%$)
Observed reflections	1289 ($F > 4.0\sigma(F)$)
Absorption correction	Semi-empirical
Min./Max. transmission	0.5184/0.5692
System used	Siemens SHELXTL PLUS (VMS)
Solution	Direct Methods
Refinement method	Full-Matrix Least-Squares
Quantity minimized	$\Sigma w(F_o - F_c)^2$
Absolute structure	n/a
Extinction correction	$\chi = 0.00052(11)$, where $F^* = F[1 + 0.002\chi F^2/\sin(2\theta)]^{-1/4}$
Hydrogen atoms	Riding model, fixed isotropic U
Weighting scheme	$w^{-1} = \sigma^2(F) + 0.002F^2$
Number of parameters refined	155
Final R indices (obs. data)	$R = 3.31\%$, $R_w = 3.24\%$
R Indices (all data)	$R = 5.14\%$, $R_w = 3.56\%$
Goodness-of-Fit	1.28
Largest and mean Δ/σ	0.305, 0.069
Data-to-parameter ratio	8.3:1
Largest difference peak	0.20 eÅ^{-3}
Largest difference hole	-0.23 eÅ^{-3}

Table 4b
Crystal data and refinement details for complex II

Empirical formula	$C_{25}H_{28}Fe_2O$
Color; Habit	Red fragment
Crystal size (mm)	$0.28 \times 0.20 \times 0.44$
Crystal system	Triclinic
Space group	$P\bar{1}$
Unit cell dimensions	$a = 9.872(4)$ Å
	$b = 11.355(4)$ Å
	$c = 19.900(7)$ Å
	$\alpha = 94.77(3)°$
	$\beta = 102.84(3)°$
	$\gamma = 105.38(3)°$
Volume	2072.9(13) Å^3
Z	4
Formula weight	456.2
Density (calc.)	1.462 Mg/m^3
Absorption coefficient	1.411 mm^{-1}
$F(000)$	952
Diffractometer used	Siemens R3m/V
Radiation	Mo-K_α ($\lambda = 0.71073$ Å)
Temperature (K)	298
Monochromator	Highly oriented graphite crystal
2θ range	3.5 to 45.0°
Scan type	ω
Scan speed	Variable; 3.00 to 20.00°/min. in ω
Scan range (ω)	1.50°
Background measurement	Stationary crystal and stationary counter at beginning and end of scan, each for 25.0% of total scan time
Standard reflections	3 measured every 100 reflections
Index ranges	$-5 \leqslant h \leqslant 10$, $-12 \leqslant k \leqslant 11$, $-21 \leqslant l \leqslant 20$
Reflections collected	5905
Independent reflections	5391 ($R_{int} = 1.16\%$)
Observed reflections	4246 ($F > 3.0\sigma(F)$)
Absorption correction	Semi-empirical
Min./Max. transmission	0.4263/0.4461
System used	Siemens SHELXTL PLUS (VMS)
Solution	Direct methods
Refinement method	Full-Matrix Least-Squares
Quantity minimized	$\Sigma w(F_o - F_c)^2$
Absolute structure	n/a
Extinction correction	$\chi = 0.00068(6)$, where $F^* = F[1 + 0.002\chi F^2/\sin(2\theta)]^{-1/4}$
Hydrogen atoms	Riding model, fixed isotropic U
Weighting scheme	$w^{-1} = \sigma^2(F) + 0.0001F^2$
Number of parameters refined	506
Final R indices (obs. data)	$R = 4.43\%$, $R_w = 3.92\%$
R Indices (all data)	$R = 6.18\%$, $R_w = 4.15\%$
Goodness-of-Fit	2.13
Largest and mean Δ/σ	1.204, 0.172
Data-to-parameter ratio	8.4:1
Largest difference peak	0.29 eÅ^{-3}
Largest difference hole	-0.29 eÅ^{-3}

filtration, the hexane was removed on a rotary evaporator. Vacuum sublimation of the residue at 50°C/0.2 mmHg removed di-n-butyl mercury. The residue was recrystallized from hexane to yield red crystals of II. Yield: 4.2 g, 9.21 mmol (83%).

Structure determination and refinement

The crystals were mounted on glass fibres for X-ray diffraction. All data were collected at room temperature on a R3m/V Nicolet four-circle diffractometer with graphite-monochromated Mo–K_α radiation; λ (Mo–K_α) = 0.71073Å. Unit cell parameters and standard deviations were obtained by least-squares fit to 25 reflections randomly distributed in reciprocal space and lying in the 2θ range of 15–30°. Intensity data were collected in the ω scan mode with scan ranges of 1.30° (I) and 1.50° (II). In both cases a variable scan speed of 3–20 degree/minute was used. Background counts were taken with stationary crystal and total background time to scan time ratio of 0.5. Three standard reflections were monitored in each case and showed no significant decay. The data were corrected for Lorentz and polarization effects and a semi-empirical absorption correction giving Min/Max Transmission ratios of 0.518/0.569 for the compound I and 0.4263/0.4461 for the compound II were applied to the raw intensity data. Full details are in Table 4.

The corresponding space groups were uniquely determined in both the compounds from their systematic absences. The structures were solved and refined using the SHELXTL-PLUS software package on a MicroVax II computer. The hydrogen atoms were placed at calculated positions (C–H 0.96 Å; U_H = 0.08) during refinements. Full-matrix least-squares refinements minimizing $\Sigma w (F_o - F_c)^2$ was carried out with anisotropic thermal parameters for non-hydrogen atoms. Selected bond angles and lengths are presented in Table 2 and 3 and atomic coordinates are given in Table 5a and 5b.

Table 5a

Atomic coordinates ($\times 10^4$) and equivalent isotropic displacement coefficients (Å$^2 \times 10^3$) for complex I

	x	y	z	U_{eq} [a]
Fe	2345(1)	2842(1)	4794(1)	40(1)
O	−2116(5)	1556(2)	3584(2)	84(1)
C(1)	950(6)	1666(2)	4697(3)	40(1)
C(2)	−183(6)	2190(2)	5356(3)	51(1)
C(3)	1378(8)	2439(3)	6117(3)	60(2)
C(4)	3471(8)	2093(3)	5936(3)	60(2)
C(5)	3235(6)	1620(2)	5074(3)	48(1)
C(6)	2370(10)	3328(3)	3432(3)	73(2)
C(7)	1068(8)	3834(3)	4015(4)	81(2)
C(8)	2470(10)	4129(2)	4786(3)	69(2)
C(9)	4582(8)	3795(3)	4688(3)	61(2)
C(10)	4517(8)	3307(3)	3857(3)	63(2)
C(11)	−237(7)	1301(2)	3816(3)	47(1)
C(12)	784(6)	622(2)	3192(3)	47(1)
C(13)	2430(8)	1038(3)	2552(3)	74(2)
C(14)	1975(9)	−64(3)	3815(3)	83(2)
C(15)	−1073(8)	223(3)	2540(4)	106(2)

[a] Equivalent isotropic U defined as one third of the trace of the orthogonalized U_{ij} tensor.

Table 5b

Atomic coordinates ($\times 10^4$) and equivalent isotropic displacement coefficients ($Å^2 \times 10^3$) for complex II

	x	y	z	U_{eq}
Fe(1)	1956(1)	−3205(1)	4427(1)	47(1)
Fe(2)	1826(1)	1258(1)	3432(1)	39(1)
O(1)	196(3)	−829(3)	4522(1)	48(1)
C(1)	268(5)	−2636(4)	3866(2)	35(2)
C(2)	−228(5)	−3544(4)	4280(2)	42(2)
C(3)	115(5)	−4633(4)	4071(3)	52(2)
C(4)	846(6)	−4410(4)	3547(3)	58(2)
C(5)	943(5)	−3189(4)	3415(2)	46(2)
C(6)	3234(7)	−3851(6)	5159(4)	91(3)
C(7)	3972(6)	−3425(7)	4671(4)	92(4)
C(8)	4083(6)	−2149(6)	4671(3)	76(3)
C(9)	3396(6)	−1810(5)	5170(3)	65(2)
C(10)	2895(6)	−2855(7)	5477(3)	82(3)
C(11)	1051(5)	−613(4)	3478(2)	35(2)
C(12)	2561(5)	−121(4)	3833(3)	45(2)
C(13)	3336(5)	380(4)	3349(3)	52(2)
C(14)	2328(5)	205(4)	2704(3)	51(2)
C(15)	924(5)	−392(4)	2778(2)	42(2)
C(16)	551(6)	2408(4)	3245(3)	57(2)
C(17)	892(6)	2309(4)	3958(3)	57(2)
C(18)	2415(6)	2730(4)	4207(3)	58(2)
C(19)	3013(6)	3078(4)	3649(3)	55(2)
C(20)	1872(6)	2878(4)	3058(3)	55(2)
C(21)	−61(5)	−1403(4)	3819(2)	34(2)
C(22)	−1707(5)	−1641(4)	3424(2)	45(2)
C(23)	−2051(5)	−431(4)	3292(3)	58(2)
C(24)	−2124(5)	−2529(5)	2733(3)	58(2)
C(25)	−2701(5)	−2250(5)	3873(3)	69(3)
Fe(3)	3574(1)	6853(1)	8351(1)	44(1)
Fe(4)	2181(1)	6842(1)	10963(1)	46(1)
O(2)	3959(3)	8892(3)	9980(2)	48(1)
C(26)	2466(4)	7168(4)	9099(2)	35(2)
C(27)	3364(5)	6393(4)	9295(2)	46(2)
C(28)	2927(6)	5325(4)	8785(3)	56(2)
C(29)	1760(6)	5435(5)	8263(3)	59(2)
C(30)	1475(5)	6554(4)	8444(2)	46(2)
C(31)	5057(7)	8404(6)	8241(4)	77(3)
C(32)	5746(6)	7485(7)	8414(3)	75(3)
C(33)	5085(7)	6456(6)	7889(3)	70(3)
C(34)	4005(7)	6731(6)	7396(3)	75(3)
C(35)	3989(7)	7934(7)	7611(3)	80(3)
C(36)	1700(4)	7799(4)	10142(2)	35(2)
C(37)	1764(5)	8457(4)	10797(2)	51(2)
C(38)	720(6)	7740(5)	11094(3)	56(2)
C(39)	8(5)	6629(5)	10633(3)	49(2)
C(40)	617(4)	6652(4)	10055(2)	38(2)
C(41)	3305(7)	5576(6)	10925(3)	68(3)
C(42)	4264(6)	6766(6)	11131(3)	71(3)
C(43)	4021(8)	7265(7)	11742(3)	94(4)
C(44)	2913(9)	6372(9)	11906(3)	98(4)
C(45)	2467(7)	5331(7)	11400(4)	85(3)
C(46)	2478(4)	8277(4)	9597(2)	36(2)
C(47)	1797(5)	9257(4)	9240(2)	46(2)
C(48)	2475(6)	9689(5)	8652(3)	65(3)
C(49)	2092(6)	10420(4)	9772(3)	63(2)
C(50)	137(5)	8730(5)	8961(3)	62(2)
H(1)	302	−217	4576	50
H(2)	4276	8981	9755	50

Acknowledgments

Supplementary materials available. Tables of complete bond lengths and bond angles, anisotropic thermal parameters, listings of observed and calculated structure factors are available from the authors.

This research has been supported by the Robert A. Welch Foundation, Houston, Texas, and the National Science Foundation, RII-88-02973 *via* establishment of a Minority Research Center of Excellence in Materials Science.

References

1 H.K. Sharma, S.P. Vincenti, R. Vicari, F. Cervantes-Lee and K.H. Pannell, Organometallics, 9 (1990) 2109.
2 H.K. Sharma, F. Cervantes-Lee and K.H. Pannell, J. Organomet. Chem., 409 (1991) 321.
3 W. Bell and C. Glidewell, J. Chem. Res. (S), (1991) 44.
4 M.J. Reuter and R. Damrauer, J. Organomet. Chem., 82 (1974) 201.
5 Q. Liu, Y. Hu, F. Li and J. Huang, Wuli Huaxue Xuabao, 2 (1986) 68.
6 Y-P. Wang J-M. Hwu, J. Organomet. Chem., 390 (1990) 179.
7 J.C. Barnes, W. Bell, C. Glidewell and R.A. Howie, J. Organomet. Chem., 385 (1990) 369.
8 D.S. Trifan and R. Backsai, J. Am. Chem. Soc., 82 (1960) 5010.
9 (a) E.S. Shubina, L.M. Epstein, A.I. Yanovsky, T.V. Timofeeva, Y.T. Struchkov, A.Z. Kreindlin, S.S. Fadeeva and M.I. Rybinskaya, J. Organomet. Chem., 345 (1988) 313; (b) E.S. Shubina, L.M. Epstein, T.M. Timofeeva, Yu.T. Struchkov, A.Z. Kreindlin, S.S. Fadeeva and M.I. Rybinskaya, J. Organomet. Chem., 346 (1988) 59; (c) E.S. Shubina, L.M. Epstein, T.V. Timofeeva, Y.T. Struchkov, A.Z. Kreindlin, S.S. Fadeeva and M.I. Rybinskaya, J. Organomet. Chem., 401 (1991) 133; (d) E.S. Shubina, L.M. Epstein, A.Z. Kreindlin, S.S. Fadeeva and M.I. Rybinskaya, J. Organomet. Chem., 401 (1991) 145; (e) E.S. Shubina, L.M. Epstein, Y.L. Slovokhotov, A.V. Mironov, Y.T. Struchkov, V.S. Kaganovich, A.Z. Kreindlin and M.I. Rybinskaya, J. Organomet. Chem. 401 (1991) 155.
10 D. Seyferth, H.P. Hofmann, R. Burton and J.F. Helling, Inorg. Chem. 1 (1962) 227.
11 K. Yates and F. Agolini, Can. J. Chem. 44 (1966) 2229.
12 J.P. Amoureux, M. Bee, C. Gors, V. Warin and F. Baert, Cryst. Struct. Comm., 8 (1979) 449.
13 W.C. Herndon and T.P. Radhakrishnan, Chem. Phys. Lett. 148 (1988) 492.
14 M.P. Gupta and T.N.P. Gupta, Acta Crystallogr., Sect. B, 31 (1975) 7.
15 R. Karlsson, Acta Cryst., B32 (1976) 2609.
16 J.A. McMillan and I.C. Paul, Tetrahedron Lett., (1976) 4219.
17 T. Kovacs, L. Parkanyi, I. Pelczer, F. Cervantes-Lee, K.H. Pannell and P.F. Torrence, J. Med. Chem., 34 (1991) 2595.